Title
Increased autophagy accelerates colchicine-induced muscle toxicity.

Journal
Autophagy, 9(12)

ISSN
1554-8635

Authors
Ching, James K
Ju, Jeong Sun
Pittman, Sara K
et al.

Publication Date
2013-10-29

Increased autophagy accelerates colchicine-induced muscle toxicity

James K. Ching[1], Jeong Sun Ju[1], Sara K. Pittman[1], Marta Margeta[2] and Conrad C. Weihl[1]

[1]Department of Neurology, Hope Center for Neurological Diseases, Washington University School of Medicine, St Louis, MO 63110, USA; [2] Department of Pathology, University of California San Francisco School of Medicine, San Francisco, CA 94143, USA

This article has been published in Autophagy 9(12), doi.org/10.4161/auto.26150. The link to the final version of the article is: https://www.landesbioscience.com/journals/autophagy/article/26150/.

Correspondence to: Conrad C. Weihl (weihlc@neuro.wustl.edu), Department of Neurology, Washington University School of Medicine, PO Box 8111, 660 South Euclid Avenue, St Louis, MO 63110, USA. Tel: (314) 362-6981; Fax: (314) 362-3752

Abbreviations: HMG-CoA, 3-hydroxy-3-methylglutaryl-coenzyme A; HMGCR, 3-hydroxy-3-methylglutaryl-CoA reductase; IBMPFD, inclusion body myopathy associated with Paget disease of the bone and fronto-temporal dementia; i.p., intraperitoneal; PBS, phosphate-buffered saline; TA, tibialis anterior

Abstract:

Colchicine treatment is associated with an autophagic vacuolar myopathy in human patients. The presumed mechanism of colchicine-induced myotoxicity is the destabilization of the microtubule system that leads to impaired autophagosome-lysosome fusion and the accumulation of autophagic vacuoles. Using the MTOR inhibitor rapamycin we augmented colchicine's myotoxic effect by increasing the autophagic flux; this resulted in an acute myopathy with muscle necrosis. In contrast to myonecrosis induced by cardiotoxin, myonecrosis induced by a combination of rapamycin and colchicine was associated with accumulation of autophagic substrates such as LC3-II and SQSTM1; as a result, autophagic vacuoles accumulated in the center of myofibers, where LC3-positive autophagosomes failed to colocalize with the lysosomal protein marker LAMP2. A similar pattern of central LC3 accumulation and myonecrosis is seen in human patients with colchicine myopathy, many of whom have been treated with statins (HMGCR/HMG-CoA reductase inhibitors) in addition to colchicine. In mice, cotreatment with colchicine and simvastatin also led to muscle necrosis and LC3 accumulation, suggesting that, like rapamycin, simvastatin activates autophagy. Consistent with this, treatment of mice with four different statin medications enhanced autophagic flux in skeletal muscle *in vivo*. Polypharmacy is a known risk factor for toxic myopathies; our data suggest that some medication combinations may simultaneously activate upstream autophagy signaling pathways while inhibiting the degradation of these newly synthesized autophagosomes, resulting in myotoxicity.

Keywords: Autophagy; toxic myopathy, colchicine, HMG-CoA reductase inhibitor; vacuolar myopathy

Introduction

Most cases of toxic myopathy are the consequence of drugs commonly used for therapeutic interventions.[2] Muscle tissue is particularly vulnerable to drug-associated toxicity because of its relative abundance, high blood flow and metabolic rate. One example of a toxic myopathy is colchicine-induced myopathy.[3] Colchicine is commonly used for the treatment of gouty arthritis, often at high initial doses. Colchicine myopathy is characterized by myalgias, muscle weakness and occasional rhabdomyolysis.[3] In addition to myopathy, muscle tissue demonstrates the accumulation of autophagic vacuoles.[3] The mechanism of colchicine-associated muscle toxicity is poorly understood. Colchicine destabilizes microtubules, which are required for both endosomal and autophagosomal maturation,[4] the resultant accumulation of endosomal and autophagic debris has been previously proposed as the pathogenic mechanism for colchicine myopathy.[4]

Macroautophagy (autophagy) is the bulk degradation of cytoplasmic proteins and organelles.[5] This process includes multiple steps, many of which require intact microtubules: 1) phagophore initiation and expansion, 2) autophagosome formation and 3) autophagosome fusion with acidic lysosomes.[6] Skeletal muscle is sensitive to stimuli that activate autophagic degradation, such as nutrient deprivation and exercise.[7, 8] In addition, several drugs such as rapamycin activate autophagy in mouse skeletal muscle.[9] If the accumulation of autophagic debris due to impaired microtubule trafficking is indeed the pathogenic mechanism of colchicine-induced myopathy, it would be reasonable to expect that inducing autophagy in the setting of colchicine treatment should exacerbate the disease pathology/progression.

Statins [HMGCR (3-hydroxy-3-methylglutaryl-CoA reductase) inhibitors] are among the most commonly prescribed medications for the reduction of cholesterol,[10] but their use is limited by muscle toxicity. Statin use has been associated with muscle pain, exercise intolerance, muscle weakness and rhabdomyolysis.[11] Interestingly, the risk of statin-associated muscle toxicity increases with age and medication usage.[11] In fact, many acute cases of muscle toxicity

have been reported in patients concomitantly taking statins and colchicine.[12-21] Statins reportedly induce autophagy *in vitro,*[22, 23] lending credence to our hypothesis that active autophagy is the potential driving force behind colchicine-induced muscle toxicity. To explore the impact of enhanced autophagy in colchicine-induced myopathy, we evaluated muscle pathology in mice treated with rapamycin or simvastatin in the setting of colchicine.

Results

Rapamycin accelerates colchicine-induced muscle toxicity.

Previous studies have evaluated the toxicity of colchicine in a rodent model and found that four weeks of intraperitoneal (i.p.) colchicine at a dose of 0.4 mg/kg/d caused a vacuolar myopathy.[4] Similarly, we found that i.p. colchicine at the same dose for 40 d caused myopathy with rare vacuoles, and the accumulation of autophagic markers LC3 and SQSTM1 in mouse skeletal muscle (**Fig. 1**; see **Fig. S1** for isotype control IgG staining). In some cases, LC3 and SQSTM1 colocalized to the central region of a myofiber (**Fig. 1E**). To investigate whether autophagy induction accelerated colchicine-induced muscle toxicity, we treated 24 mice for 10 d with vehicle, i.p. colchicine (0.4 mg/kg/d), i.p. rapamycin (10 mg/kg/d) or i.p. colchicine and rapamycin combination; following treatment, we analyzed the tibialis anterior (TA) and quadriceps muscles by routine histochemistry. TA and quadriceps muscles from mice treated for 10 d with colchicine or rapamycin alone appeared similar to control mouse muscle when visualized via hematoxylin and eosin or congo red, with no evidence of myopathic features (not shown). Therefore, in the case of colchicine, treatment periods longer than 10 d are necessary to induce the vacuolar changes seen in colchicine myopathy. In contrast, mice treated with 0.4 mg/kg/d i.p. colchicine and 10 mg/kg/d i.p. rapamycin for 10 d showed abnormal fibers with rare vacuolar structures, as evidenced by hematoxylin and eosin, congo red, acid phosphatase and succinate dehydrogenase staining (**Fig. 2A-D**). To confirm that the observed abnormal fibers were necrotic and that we had indeed accelerated the muscle toxicity induced by colchicine, we

immunostained muscle sections with an antibody to complement c5b9, a marker of necrotic muscle fibers (**Fig. 2E-H**). The percentage of fibers that stained positive for c5b9 increased significantly in mice treated with both drugs compared to vehicle-, rapamycin-, or colchicine-treated groups (**Fig. 2I**). These data suggest that enhancing autophagy with rapamycin augments the pathogenesis of colchicine, leading to a necrotic autophagic myopathy.

Colchicine plus rapamycin-treated mouse muscle accumulates autophagic structures. Given that we enhanced autophagosome biogenesis with rapamycin and at the same time blocked autophagosome degradation with colchicine, we reasoned that the pathological changes seen in the skeletal muscle of colchicine plus rapamycin-treated mice may be due to the accumulation of nondegraded autophagosomes. To test this hypothesis, we immunoblotted TA muscle lysates from vehicle-, rapamycin-, colchicine- or colchicine plus rapamycin-treated mice for the autophagic substrates SQSTM1 and LC3 (**Fig. 3A**). Upon phagophore formation, LC3-I can become lipidated and attach to the growing phagophore membrane as LC3-II.[7] SQSTM1 and LC3-II levels were increased in colchicine-treated mice and to a greater extent in colchicine plus rapamycin-treated mouse muscle (**Fig. 3A**). Ubiquitinated proteins can be degraded via autophagy and are thus autophagic substrates.[5] Consistent with this, the level of ubiquitinated proteins was elevated in colchicine plus rapamycin-treated mouse muscle (**Fig. 3A**). In addition, two other autophagic proteins, BNIP3 and BECN1/Beclin1, were increased in TA muscle lysates from mice treated with both colchicine and rapamycin compared to mice treated with vehicle, rapamycin alone, or colchicine alone (**Fig. 3A**). The accumulation of autophagic substrates such as LC3-II and SQSTM1 may not solely be caused by a decrease in their degradation but also as a result of enhanced transcription of the corresponding genes. To test this, we performed quantitative RT-PCR expression analysis using total RNA isolated from TA muscle obtained from vehicle-treated and colchicine plus rapamycin-treated mice (**Fig. 3B**). Consistent with enhanced autophagosome biogenesis, the expression of MAP1LC3A,

MAP1LC3B and SQSTM1 were increased by ~3-4 fold (**Fig. 3B**). In addition, the expression of the lysosomal/endosomal protein LAMP1 was increased by ~3 fold (**Fig. 3B**). In contrast, the expression of BNIP3 was not different between groups (**Fig. 3B**).

We do not think that the accumulation of autophagic substrates was a consequence of muscle necrosis, since muscle treated for two days with cardiotoxin showed a modest change in LC3-II levels and a decrease in SQSTM1 levels (**Fig. 3C**). Immunohistochemical staining of LC3, SQSTM1 and BNIP3 in cardiotoxin-treated muscle demonstrated that these autophagic markers were indeed altered in myofibers and not infiltrating cells (**Fig. S2**). Interestingly, BECN1 and BNIP3, as well as the necrotic signaling kinase RIPK1, were elevated after two days of cardiotoxin-induced muscle injury (**Fig. 3C**).

To define the localization of accumulated autophagic proteins in treated mouse muscle, we performed immunohistochemistry with antibodies to LC3, SQSTM1 and BNIP3; in addition, we used an antibody to the lysosomal marker, LAMP2. All autophagic markers were increased in colchicine plus rapamycin-treated mouse muscle when compared to muscle from the control, rapamycin-, and colchicine-treated mice (**Fig. 3D** and not shown). Scattered fibers showed an increase in SQSTM1-positive puncta in colchicine alone-treated muscle, but other autophagic markers were not increased above that seen with vehicle or rapamycin treatment (**Fig. 3D**). Interestingly, these autophagic proteins were localized to the central region of myofibers (**Fig. 4**) rather than throughout the sarcoplasm, as seen in cardiotoxin-treated muscle (**Fig. S2**). To further characterize this, we performed several immunofluorescence colocalization studies. As expected, LC3 and LAMP2 did not colocalize in colchicine plus rapamycin-treated mouse muscle, consistent with a failure in autophagosome-lysosome fusion (**Fig. 5A**). In contrast, SQSTM1 colocalized with LC3, suggesting that the loading of autophagosomes was not impaired (**Fig. 5B**). Finally, SQSTM1 and ubiquitinated proteins strongly colocalized, indicating that association of SQSTM1 with ubiquitinated substrates was not affected (**Fig. 5C**). Electron microscopy of similarly treated muscle demonstrated the accumulation of vacuolated structures,

many of which had double membranes and contained cellular contents, consistent with autophagosomes. These structures were found within the central region of fibers between myofibrils (**Fig. 5D-E**).

Simvastatin-induced autophagy accelerates colchicine-induced muscle toxicity.

We previously reported the pathological features of 7 patients with colchicine-associated myopathy.[24] Polypharmacy is a well-established risk factor for colchicine muscle toxicity,[3] and commonly prescribed drugs, such as the cholesterol lowering agents statins, are likely to play an important role. Indeed, 2 of 7 patients in our original patient cohort (#22 and #25) and 2 of 2 patients diagnosed with colchicine myopathy since completion of that study (4 of 9 or 44% in total) were on both colchicine and a statin at the time of muscle biopsy. Immunohistochemical staining of these patients' muscle biopsies showed a pattern of LC3 and SQSTM1 deposition in myofibers similar to that seen in colchicine plus rapamycin-treated mice (a representative biopsy is shown in **Fig. 6**; compare with a muscle sample from control patient with no muscle disease, **Fig. S3**). A detailed quantification of the percentage of LC3- and SQSTM1-immunopositive myofibers in these human specimens has been previously reported.[24] We therefore reasoned that statin medications, like rapamycin, may accelerate and/or potentiate colchicine toxicity.

To test this, mice were divided into 4 treatment groups of 6 mice each: vehicle alone, 0.4 mg/kg/d colchicine, 10 mg/kg/d simvastatin, or both colchicine and simvastatin daily for 10 d. Following treatment, mice were sacrificed and TA and quadriceps muscles were analyzed via western blot, routine histopathology and immunohistochemistry. Similar to the muscle pathology seen in mice treated with colchicine plus rapamycin (**Fig. 2 and 3**) and human muscle pathology in patients treated with colchicine plus statin (**Fig. 6**), muscle from mice treated with colchicine plus simvastatin displayed myopathic features, with scattered necrotic fibers and LC3 accumulation within the center of myofibers (**Fig. 7B and 7D**). This pattern was not seen in the other treatment groups, including the group treated with simvastatin alone (**Fig. 7A and 7C**). To

confirm necrosis and quantify the augmentation of colchicine toxicity by simvastatin, we immunostained tissue with an antibody to c5b9 and quantified the percentage of positive fibers (**Fig. 7E, F**). Similar to colchicine plus rapamycin, colchicine plus simvastatin treatment resulted in an increase in necrotic fibers when compared with vehicle-, colchicine- or simvastatin-treated mice (**Fig. 7G**). Immunoblotting for autophagic substrates in colchicine plus simvastatin-treated mouse muscle also demonstrated an increase in LC3-II, SQSTM1, and ubiquitinated proteins when compared to any of the control groups (**Fig. 7H**); these data raise the possibility that, like rapamycin, statins activate autophagy.

Statins induce autophagy in mouse skeletal muscle.

Previous studies have demonstrated that statins can induce autophagy in cell culture models of skeletal muscle,[22, 23] but it has not been established whether this occurs *in vivo* in mature skeletal muscle. To evaluate this, we treated mice with 4 different statin drugs (simvastatin, atorvastatin, lovastatin, and pravastatin) for 7 d prior to isolating skeletal muscle and performing an immunoblot using an anti-LC3 antibody. To confirm that these drugs truly enhanced autophagic flux, we treated similar mice with 0.4 mg/kg colchicine on days 6 and 7 and then harvested TA muscles for immunoblot. LC3-II levels were unchanged in muscle from mice treated with statins alone when compared with muscle from vehicle-treated mice. As we have previously demonstrated, there was accumulation of LC3-II in mice that received colchicine for 2 d, indicating a block in basal autophagy (**Fig. 8A, B**).[9] Consistent with an increase in autophagic flux, skeletal muscle lysates from mice receiving a statin for 7 d and colchicine on days 6 and 7 displayed increased accumulation of LC3-II when compared to the colchicine group, suggesting that statins enhance autophagic flux *in vivo.*[9] The increase in flux is represented as the ratio of LC3-II to actin from 4 mice per condition (**Fig. 8B**).

Discussion

The myotoxic effect of colchicine is well known, but it has been difficult to pinpoint its pathogenic mechanism. The bulk of the relevant mechanisms proposed so far to explain colchicine-induced muscle toxicity hinges on the disruption of the microtubule network.[3, 4] In this study, we report data which support an expansion of the paradigm regarding the mechanism of colchicine-induced muscle toxicity from mere disruption of microtubule network to a functional and/or synergistic relationship between colchicine and autophagy induction. We have shown that mice treated for 10 d with both colchicine and autophagic inducers such as rapamycin or simvastatin display (1) increased accumulation of autophagic substrates and ubiquitinated proteins; and (2) worsening of the colchicine-induced muscle pathology when compared to mice injected with colchicine alone. Thus, the emerging hypothesis is that colchicine-induced muscle toxicity is a result of autophagic vacuole build-up due to enhanced autophagosome formation and impaired autophagic degradation; this possibility is supported by the fact that autophagic markers LC3 and SQSTM1 robustly accumulate in the muscle of patients with colchicine-induced autophagic vacuolar myopathy.[24]

Colchicine and chloroquine have both been associated with toxic vacuolar myopathies.[2] In the case of chloroquine, lysosomal de-acidification is the presumed mechanism by which autophagic vacuoles accumulate and fail to be degraded.[25] Previous rodent models of chloroquine-induced myopathy have treated mice for several weeks with chloroquine to induce pathology.[26] Interestingly, dennervation of muscle hastens the development of an autophagic myopathy resulting in pathology over the course of days rather than weeks.[26] Dennervation is a potent inducer of muscle atrophy and autophagy,[9, 27, 28] an increase in autophagy in the setting of impaired autophagic degradation may explain the synergism between chloroquine treatment and dennervation in experimental models of chloroquine myopathy.

Many vacuolar myopathies are due to mutations in proteins associated with lysosomal function and accumulate autophagic proteins within the myofiber similarly to the pathology seen

in colchicine-associated myopathy. For example, Danon disease, Pompe disease and X-linked myopathy with excessive autophagy all accumulate autophagic debris.[29] Whether the activation of autophagy is beneficial or detrimental for these diseases is not known. We recently demonstrated that enhancing autophagy with rapamycin worsened the vacuolar pathology, protein aggregate accumulation and weakness in a mouse model of inclusion body myopathy associated with Paget disease of the bone and fronto-temporal dementia (IBMPFD).[1] IBMPFD is caused by mutations in valosin containing protein, which is required for maturation of autophagosomes to autolysosomes.[30] Interestingly, in the case of IBMPFD, X-linked myopathy with excessive autophagy and sporadic inclusion body myositis, MTORC1 activity is diminished, suggesting enhanced autophagosome formation.[1, 31, 32] The current study lends further support to a mechanism of disease in which activation of autophagy drives the vacuolar pathology in some myopathies.

Statins initiate autophagy in cultured cells.[22, 33] The mechanism by which statins induce autophagy likely relates to their mechanism of action within the HMGCR pathway. Specifically, depletion of geranylgeranyl diphosphate by statins and bisphosphonates can induce autophagy.[22, 34] Moreover, farnesyl transferase inhibitors and geranylgeranyl transferase inhibitors both induce autophagy *in vitro.*[35, 36] Our studies confirm these cell culture models and demonstrate that statins can effectively enhance autophagic flux *in vivo* in mouse skeletal muscle. In this context, it is worth noting that UCSF muscle pathology practice has seen a sharp increase in the number of colchicine and hydroxychloroquine myopathy cases in the last 5-6 years, coinciding with a large increase in statin use [based on a CDC survey entitled “Health, United States, 2010”, the percentage of statin-using adults (≥ 45 years of age) increased from 2% in the period of 1988-1994 to 25% in the period 2005-2008, and is likely even higher today].

Risk factors for statin muscle toxicity are higher dosages, concomitant use of certain drugs that can inhibit statin metabolism, and more recently polymorphisms in the gene *SLCO1B1/OATP1B1* that encodes solute carrier organic anion transporter family, member 1B1,

and mediates the uptake of various drugs including statins.[37, 38] It is conceivable that the accelerated muscle pathology seen in our studies is due to increased statin drug concentration in the setting of colchicine administration. However, based on the findings of our study, we propose that mutations or polymorphisms in genes within the autophagy pathway may also be risk factors for statin myotoxicity.

Materials and Methods

Antibodies and reagents for mouse studies. Antibodies for BECN1 (Cell Signaling Technologies, 3738), GAPDH (Cell Signaling Technologies, 2118), LAMP2 (Santa Cruz Biotechnology, sc-18822), BNIP3 (Abcam, ab10433), Actin (Sigma, A2066), LC3B (Sigma, L7543) for western blotting, LC3 (Nanotools, 0231-100/LC3-5F10) for immunostaining, RIPK1/RIP1 (BD Transduction Laboratories, 610458), c5b9 (Dako, M0777) and antibodies to SQSTM1 (Proteintech,18420-1-AP) for western blotting and to SQSTM1 (Sigma, P0067) for immunostaining were obtained from the indicated sources. For the autophagic assessment of necrotic fibers in Figure S2, the VECTOR M.O.M. immunodetection Kit Flourescein (Vector Laboratories, FMK-2001) was used to quench endogenous background IgG. Rapamycin (LC laboratories R-5000) and cardiotoxin (Sigma, C9759) were also purchased. Simvastatin (1965), atorvastatin (3776), lovastatin (1530), and pravastatin (2318) were obtained from TOCRIS.

Animals and drug treatments. All experiments were conducted using 3-4 month old C57BL/6 mice from Jackson Laboratory. Animal studies were approved by the Animal Studies Committee of Washington University School of Medicine. Upon arrival, mice were housed in a temperature-controlled environment with 12 h light/dark cycles, where they received food and water ad libitum. All drugs were injected intraperitoneally. Rapamycin was dissolved in 100% ethanol at 62.5 mg/ml, stored at -20°C, and diluted to 2.5 mg/ml in vehicle (5% PEG 400, 5% Tween 80 and 4% ethanol) just before injection. Colchicine was dissolved in water, stored at -20°C as a stock solution at a concentration of 4 mg/ml, and diluted to 0.1 mg/ml before injection. Simvastatin, atorvastatin, lovastatin, and pravastatin were administered at a dose of 10 mg/kg body weight. Simvastatin and lovastatin were dissolved in 100% ethanol and stored at -20°C as stocks; on the day of experiment, they were diluted with PBS immediately prior to injection. Atorvastatin was dissolved in DMSO and stored as stock solution, which was diluted with PBS immediately prior to injection. Pravastatin was dissolved in water. For all drug treatments,

control mice received equal volumes of respective vehicles. Mice were subjected to i.p. injection of both rapamycin (10 mg/kg body weight) and colchicine (0.4 mg/kg body weight) daily for 10 d. Age-match littermates were injected with vehicle (5% Tween 80, 5% polyethylene glycol, and 4% ethanol), rapamycin alone, or colchicine alone as controls. Similar experiments were performed with simvastatin (10 mg/kg body weight) in place of rapamycin. Cardiotoxin (from *Naja mossabica mossambica)* was dissolved in water and stored at -20°C as stock solution, which was diluted in PBS to a working concentration of 12 μM prior to experiment. For each mouse, tibialis anterior muscles were injected with 100 μL of 12 μM cardiotoxin and muscles were harvested 2 d later.

Western blotting. Muscle tissues were homogenized using RIPA lysis buffer (50 mM Tris-HCl, pH 7.4, 150 mM NaCl, 1% NP-40, 0.25% Na-deoxycholate, 1 mM EDTA) supplemented with protease inhibitor cocktail (Sigma-Aldrich, s8820-20TAB) and then centrifuged at 14,000 g for 10 min. Protein concentrations were determined using BCA protein assay kit (Thermo Fisher Scientific, 23225). Aliquots of lysates were solubilized in Laemmli sample buffer and equal amounts of proteins were separated by 12% SDS-PAGE. Proteins were transferred to nitrocellulose membrane and the membrane was blocked with 5% nonfat dry milk in phosphate-buffered saline (PBS) for 1 h. The membrane was then incubated with primary antibodies in 5% nonfat dry milk overnight at 4°C; after incubation with the appropriate secondary antibody conjugated with horseradish peroxidase, enhanced chemiluminescence (ImmunoPure, 31430) was used for protein detection. If necessary, blots were stripped using Re-blot strong solution (Millipore, 2504) and reprobed with the appropriate antibodies. Autoradiographs of immunoblots were scanned using an Epson 636 Expression scanner; immunoblots were obtained using the G:BoxChemi XT4, Genesys Version 1.1.2.0 (Syngene).

Gene expression analyses. Total RNA was isolated from TA muscle with SV Total RNA isolation kit (Promega, Z3100) according to the manufacturer's instructions. The concentration and quality of the total RNA isolated was determined using a Nanodrop spectrophotometer. cDNA was synthesized using the RT^2 First Strand kit (Qiagen, 330401). Gene expression levels were analyzed by real-time PCR on an Applied Biosystems model 7500 (software v2.0.5) using the RT^2 SYBER Green ROX qPCR mastermix (Qiagen, 330522) and the mouse autophagy RT^2 Profiler PCR array (Qiagen, 330231 PAMM-084ZA), which contains primers for the expression of 84 autophagy genes arranged in a staggered format. Data were normalized to the average of 4 housekeeping genes, *Gapdh*, *Actb/β-actin*, *B2m/β2-microglobulin* and *Gusb/β-glucoronidase* and expressed in terms of $2^{-\Delta\Delta CT}$.

Histochemistry, immunohistochemistry and electron microscopy. Isolated muscle was mounted using tragacanth gum (Sigma, G1128) and quick frozen in liquid nitrogen-cooled 2-methylbutane. Samples were stored at -80°C until sectioning into 10-μm sections. Hematoxylin and eosin, congo red, acid phosphatase and succinate dehydrogenase staining was performed as previously described.[39] Briefly, muscle sections were affixed to slides incubated for 10 min in ice-cold acetone, mounted with Prolong Gold + DAPI (Invitrogen, P36931), and examined using a fluorescence microscope [Nikon 80i upright+ and Roper Scientific EZ monochrome CCD camera with deconvolution software analysis (NIS Elements, Nikon)]. Nonfluoresent images were taken with a 5 megapixel color CCD (Nikon). For electron microscopy, TA muscle was harvested, rinsed briefly in PBS and then placed immediately in Karnovsky fixative[40] at 4°C for 24 h. Fixed muscle was embedded in plastic and sectioned for EM imaging. Images were taken using a Jeol 1400 and a Gatan Orius 832 Digital Camera. Image processing and analysis were done with (NIS Elements 4.0) software and Adobe Photoshop.

Quantification of necrotic fibers. The percentage of c5b9-positive fibers was quantified per 20X field. 20 randomly selected microscopy fields from 10 TA muscles from 5 mice/condition were selected and the total number of myofibers and the number of immunoreactive fibers were counted and expressed as a percentage.

Human subjects. Study design was reviewed and approved by the University of California San Francisco Committee on Human Research; the informed consent requirement was waived given the noninvasive nature of the study and a minimal potential for harm to study participants. Immunoperoxidase staining for LC3 (mouse monoclonal antibody, clone 5F10, Nanotools, 0231-100) and SQSTM1 (guinea pig polyclonal antibody, Progen Biotechnik, GP62) was performed on formalin-fixed, paraffin-embedded tissue samples using the Ventana Benchmark XT automated slide preparation system as described previously.[24] Images were taken with a DP72 digital camera on a BX41 bright-field light microscope using cellSens Entry 1.6 software (all by Olympus) and were edited with Adobe Photoshop CS5 Version 12.1.32.

Acknowledgements: We thank Dr. Alan Pestronk for helpful discussions and Dr. Han S. Lee for help with analysis of human subject clinical data. Dr. Weihl is funded by the NIH R01-AG031867, K02-AG042095 and the Muscular Dystrophy Association. Dr. Margeta is supported by NIH R01-NS073765 and UCSF REAC Award.

References:

1. Ching JK, Elizabeth SV, Ju JS, Lusk C, Pittman SK, Weihl CC. mTOR dysfunction contributes to vacuolar pathology and weakness in valosin-containing protein associated inclusion body myopathy. Hum Mol Genet 2013.
2. Dalakas MC. Toxic and drug-induced myopathies. Journal of neurology, neurosurgery, and psychiatry 2009; 80:832-8.
3. Wilbur K, Makowsky M. Colchicine myotoxicity: case reports and literature review. Pharmacotherapy 2004; 24:1784-92.
4. Kuncl RW, Bilak MM, Craig SW, Adams R. Exocytotic "constipation" is a mechanism of tubulin/lysosomal interaction in colchicine myopathy. Experimental cell research 2003; 285:196-207.
5. Rubinsztein DC, Marino G, Kroemer G. Autophagy and aging. Cell 2011; 146:682-95.
6. Ravikumar B, Acevedo-Arozena A, Imarisio S, Berger Z, Vacher C, O'Kane CJ, et al. Dynein mutations impair autophagic clearance of aggregate-prone proteins. Nat Genet 2005; 37:771-6.
7. Sandri M. Autophagy in skeletal muscle. FEBS Lett 2010; 584:1411-6.
8. He C, Bassik MC, Moresi V, Sun K, Wei Y, Zou Z, et al. Exercise-induced BCL2-regulated autophagy is required for muscle glucose homeostasis. Nature 2012; 481:511-5.
9. Ju JS, Varadhachary AS, Miller SE, Weihl CC. Quantitation of "autophagic flux" in mature skeletal muscle. Autophagy 2010; 6.
10. Taylor F, Huffman MD, Macedo AF, Moore TH, Burke M, Davey Smith G, et al. Statins for the primary prevention of cardiovascular disease. Cochrane database of systematic reviews 2013; 1:CD004816.
11. Thompson PD, Clarkson P, Karas RH. Statin-associated myopathy. JAMA : the journal of the American Medical Association 2003; 289:1681-90.
12. Baker SK, Goodwin S, Sur M, Tarnopolsky MA. Cytoskeletal myotoxicity from simvastatin and colchicine. Muscle & nerve 2004; 30:799-802.
13. Bouquie R, Deslandes G, Renaud C, Dailly E, Haloun A, Jolliet P. Colchicine-induced rhabdomyolysis in a heart/lung transplant patient with concurrent use of cyclosporin, pravastatin, and azithromycin. Journal of clinical rheumatology : practical reports on rheumatic & musculoskeletal diseases 2011; 17:28-30.
14. Justiniano M, Dold S, Espinoza LR. Rapid onset of muscle weakness (rhabdomyolysis) associated with the combined use of simvastatin and colchicine. Journal of clinical rheumatology : practical reports on rheumatic & musculoskeletal diseases 2007; 13:266-8.
15. Sarullo FM, Americo L, Di Franco A, Di Pasquale P. Rhabdomyolysis induced by co-administration of fluvastatin and colchicine. Monaldi archives for chest disease = Archivio Monaldi per le malattie del torace / Fondazione clinica del lavoro, IRCCS [and] Istituto di clinica tisiologica e malattie apparato respiratorio, Universita di Napoli, Secondo ateneo 2010; 74:147-9.
16. Alayli G, Cengiz K, Canturk F, Durmus D, Akyol Y, Menekse EB. Acute myopathy in a patient with concomitant use of pravastatin and colchicine. The Annals of pharmacotherapy 2005; 39:1358-61.
17. Atasoyu EM, Evrenkaya TR, Solmazgul E. Possible colchicine rhabdomyolysis in a fluvastatin-treated patient. The Annals of pharmacotherapy 2005; 39:1368-9.
18. Francis L, Bonilla E, Soforo E, Neupane H, Nakhla H, Fuller C, et al. Fatal toxic myopathy attributed to propofol, methylprednisolone, and cyclosporine after prior exposure to colchicine and simvastatin. Clinical rheumatology 2008; 27:129-31.
19. Hsu WC, Chen WH, Chang MT, Chiu HC. Colchicine-induced acute myopathy in a patient with concomitant use of simvastatin. Clinical neuropharmacology 2002; 25:266-8.
20. Oh DH, Chan SQ, Wilson AM. Myopathy and possible intestinal dysfunction in a patient treated with colchicine and simvastatin. The Medical journal of Australia 2012; 197:332-3.

21. Torgovnick J, Sethi N, Arsura E. Colchicine and HMG Co-A reductase inhibitors induced myopathy-a case report. Neurotoxicology 2006; 27:1126-7.
22. Araki M, Maeda M, Motojima K. Hydrophobic statins induce autophagy and cell death in human rhabdomyosarcoma cells by depleting geranylgeranyl diphosphate. European journal of pharmacology 2012; 674:95-103.
23. Araki M, Motojima K. Hydrophobic statins induce autophagy in cultured human rhabdomyosarcoma cells. Biochemical and biophysical research communications 2008; 367:462-7.
24. Lee HS, Daniels BH, Salas E, Bollen AW, Debnath J, Margeta M. Clinical utility of LC3 and p62 immunohistochemistry in diagnosis of drug-induced autophagic vacuolar myopathies: a case-control study. PloS one 2012; 7:e36221.
25. Abdel-Hamid H, Oddis CV, Lacomis D. Severe hydroxychloroquine myopathy. Muscle & nerve 2008; 38:1206-10.
26. Kumamoto T, Ueyama H, Watanabe S, Murakami T, Araki S. Effect of denervation on overdevelopment of chloroquine-induced autophagic vacuoles in skeletal muscles. Muscle & nerve 1993; 16:819-26.
27. Mammucari C, Milan G, Romanello V, Masiero E, Rudolf R, Del Piccolo P, et al. FoxO3 controls autophagy in skeletal muscle in vivo. Cell Metab 2007; 6:458-71.
28. Zhao J, Brault JJ, Schild A, Cao P, Sandri M, Schiaffino S, et al. FoxO3 coordinately activates protein degradation by the autophagic/lysosomal and proteasomal pathways in atrophying muscle cells. Cell Metab 2007; 6:472-83.
29. Malicdan MC, Noguchi S, Nonaka I, Saftig P, Nishino I. Lysosomal myopathies: an excessive build-up in autophagosomes is too much to handle. Neuromuscul Disord 2008; 18:521-9.
30. Ju JS, Fuentealba RA, Miller SE, Jackson E, Piwnica-Worms D, Baloh RH, et al. Valosin-containing protein (VCP) is required for autophagy and is disrupted in VCP disease. J Cell Biol 2009; 187:875-88.
31. Nogalska A, D'Agostino C, Terracciano C, Engel WK, Askanas V. Impaired autophagy in sporadic inclusion-body myositis and in endoplasmic reticulum stress-provoked cultured human muscle fibers. Am J Pathol 2010; 177:1377-87.
32. Ramachandran N, Munteanu I, Wang P, Ruggieri A, Rilstone JJ, Israelian N, et al. VMA21 deficiency prevents vacuolar ATPase assembly and causes autophagic vacuolar myopathy. Acta Neuropathol 2013.
33. Parikh A, Childress C, Deitrick K, Lin Q, Rukstalis D, Yang W. Statin-induced autophagy by inhibition of geranylgeranyl biosynthesis in prostate cancer PC3 cells. The Prostate 2010; 70:971-81.
34. Wasko BM, Dudakovic A, Hohl RJ. Bisphosphonates induce autophagy by depleting geranylgeranyl diphosphate. The Journal of pharmacology and experimental therapeutics 2011; 337:540-6.
35. Pan J, Chen B, Su CH, Zhao R, Xu ZX, Sun L, et al. Autophagy induced by farnesyltransferase inhibitors in cancer cells. Cancer biology & therapy 2008; 7:1679-84.
36. Ghavami S, Mutawe MM, Schaafsma D, Yeganeh B, Unruh H, Klonisch T, et al. Geranylgeranyl transferase 1 modulates autophagy and apoptosis in human airway smooth muscle. American journal of physiology Lung cellular and molecular physiology 2012; 302:L420-8.
37. Armitage J. The safety of statins in clinical practice. Lancet 2007; 370:1781-90.
38. Group SC, Link E, Parish S, Armitage J, Bowman L, Heath S, et al. SLCO1B1 variants and statin-induced myopathy--a genomewide study. The New England journal of medicine 2008; 359:789-99.
39. Weihl CC, Miller SE, Hanson PI, Pestronk A. Transgenic expression of inclusion body myopathy associated mutant p97/VCP causes weakness and ubiquitinated protein inclusions in mice. Hum Mol Genet 2007; 16:919-28.
40. Karnovsky MJ. A formaldehyde-glutaraldehyde fixative of high osmolarity for use in electron microscopy. J Cell Biology 1965; 27:137A-8A.

Figure Legends:

Figure 1. Chronic colchicine treatment leads to an autophagic vacuolar myopathy in mouse skeletal muscle. (**A-B**) Hematoxylin and eosin of TA muscle from mice treated with (**A**) vehicle or (**B**) 0.4 mg/kg/d colchicine i.p. for 40 d. Black arrow denotes a vacuolated fiber. (**C**) TA muscle similar to (**B**), immunostained with anti-SQSTM1 or (**D**) anti-LC3 antibody. DAPI-stained nuclei are blue. White arrow denotes the accumulation of autophagic proteins. Scale bar, 50 μm. (**E**) A single myofiber co-immunostained with antibodies to LC3; SQSTM1; and merged LC3 (green) and SQSTM1 (red). Scale bar, 5 μm. The sarcolemma of some fibers is outlined.

Figure 2. Rapamycin treatment augments pathology in a mouse colchicine myopathy model. Histochemical analysis of TA muscle from mice treated with colchicine (0.4 mg/kg/d) and rapamycin (10 mg/kg/d) for 10 d. (**A-B**) congo red, (**C**) acid phosphatase and (**D**) succinate dehydrogenase staining demonstrate a myopathy with scattered necrotic fibers (arrows). (**E-H**) TA muscle from (**E**) vehicle-, (**F**) rapamycin-, (**G**) colchicine- or (**H**) colchicine plus rapamycin-treated mice immunostained with an antibody to complement c5b9; arrows denote necrotic fibers. (**I**) Quantification of the percentage of c5b9-positive fibers per 20X field in muscle from mice treated with vehicle, rapamycin, colchicine or colchicine plus rapamycin for 10 d. *denotes $p<0.05$, Student's unpaired T-test between treatment and control. N=5/condition. Scale bar, 50 μm.

Figure 3. Autophagic substrates accumulate in the muscle of colchicine plus rapamycin-treated mice. (**A**) Immunoblot using antibodies to LC3, SQSTM1, ubiquitinated proteins, BNIP3, BECN1 and actin of TA muscle from 3-4 month old mice treated i.p. with vehicle, 10 mg/kg/d rapamycin (rapa), 0.4 mg/kg/d colchicine (colch), or both drugs (colch+rapa) for 10 d. Blot is a representative of 3 independent experiments. (**B**) Quantitative PCR analysis of RNA from TA muscle obtained from 3-4 month old mice treated i.p. with vehicle (veh) or colchicine+rapamycin

(colc+rap) for 10 d. Data are represented as fold change as compared to vehicle treatment. p values were obtained from Student's unpaired T-test between treatment and control. N=3/condition. (**C**) Immunoblot using antibodies described above in addition to RIPK1 kinase and GAPDH of TA muscle injected with vehicle or 100 μL of 12 μM cardiotoxin and harvested 2 d later. (**D**) TA muscle from vehicle-, rapamycin-, colchicine-, or colchicine plus rapamycin-treated mice immunostained with an antibody to LC3 or SQSTM1. DAPI-stained nuclei are blue; the sarcolemma of some fibers is outlined. Scale bar, 50 μm.

Figure 4. Immunohistochemistry of TA muscle from mice treated with vehicle (left panels) or colchicine and rapamycin (right panels) for 10 d using an anti-CAV3/caveolin 3 antibody (green) and antibodies to LC3, LAMP2, SQSTM1 and BNIP3, all in red. Scale bar, 50 μm.

Figure 5. Autophagic structures are centrally located in the myofibers of colchicine plus rapamycin-treated mice. (**A**) A single myofiber co-immunostained with antibodies to LC3, LAMP2, and merged LC3 (green) and LAMP2 (red). (**B**) A single myofiber co-immunostained with antibodies to LC3, SQSTM1, and merged LC3 (green) and SQSTM1 (red). (**C**) A single myofiber co-immunostained with antibodies to ubiquitin, SQSTM1, and merged ubiquitin (green) and SQSTM1 (red). DAPI-stained nuclei are blue; the sarcolemma of a single fiber is outlined. Scale bar, 5 μm. (**D-E**) Electron microscopy images of TA muscle from mice treated with colchicine and rapamycin. Arrows denote autophagosomes. Scale bar, 500 nm.

Figure 6. Accumulation of autophagic debris in the muscle biopsy from a patient concurrently treated with colchicine and a statin. Hematoxylin and eosin staining of frozen tissue (**A**) and toluidine blue staining of EPON-embedded tissue (**B**) demonstrate disruption of the myofibrillary apparatus (arrows in **A**) and accumulation of the vacuolated material (arrowheads in B) in the center of myofibers. Immunohistochemistry for LC3 (**C**) or SQSTM1 (**D**) on formalin-fixed,

paraffin-embedded tissue shows that vacuolated central areas contain LC3- and SQSTM1-positive autophagic material. Scale bar, 20 μm.

Figure 7. Simvastatin treatment augments pathology in a mouse colchicine myopathy model. Hematoxylin and eosin staining of TA muscle from mice treated for 10 d with (**A**) simvastatin (10 mg/kg/d) or (**B**) colchicine (0.4 mg/kg/d) and simvastatin (10 mg/kg/d). (**C-D**) TA muscle from (**C**) simvastatin- or (**D**) colchicine plus simvastatin-treated mice immunostained with an antibody to LC3. (**E-F**) TA muscle from (**E**) simvastatin- or (**F**) colchicine plus simvastatin-treated mice immunostained with an antibody to c5b9. Open arrows denote necrotic fibers and closed arrows LC3-positive fibers. Scale bar, 50 μm. (**G**) Quantification of the percentage of c5b9-positive fibers per 20X field in muscle treated with vehicle, simvastatin, colchicine, or colchicine plus simvastatin for 10 d. * denotes $p<0.05$, Student's unpaired T-test between treatment and control. N=6/condition. (**H**) Immunoblot of TA muscle from 3-4 month old mice treated i.p. with vehicle, 10 mg/kg/d simvastatin (simv), 0.4 mg/kg/d colchicine (colch), or both drugs (colch+simv) for 10 d. Blot is a representative of 3 independent experiments.

Figure 8. Statins enhance autophagic flux in mouse muscle *in vivo*. 5 cohorts of mice were treated with vehicle or 1 of 4 different statin medications: simvastatin (simv), atorvastatin (atorva), lovastatin (lova) or pravastatin (prava) i.p., at a dosage of 10 mg/kg/d for 7 d. On days 6 and 7, some mice were also administered 0.4 mg/kg/d colchicine to block autophagosome degradation. (**A**) Immunoblots of mouse TA muscle lysates using antibodies for LC3 and actin. (**B**) Densitometric quantification of LC3-II/actin from immunoblots. (+) indicates with colchicine treatment. * denotes $p<0.05$, Student's unpaired T-test between treatment and colchicine groups. N ≥ 4 mice/condition.

Figure S1. (**A**) Isotype control mouse IgG and (**B**) rabbit IgG immunostaining of TA mouse muscle. DAPI-stained nuclei are blue; scale bar is 100 μm.

Figure S2. Immunofluorescence of TA muscle 1 day following injection with (**A**,**C**, and **E**) 100 μL of PBS (vehicle) or (**B**, **D**, and **F**) 100 μL of 12 μM cardiotoxin using anti-LC3 (**A**-**B**), anti-SQSTM1 (**C**-**D**), or anti-BNIP3 (**E**-**F**) antibodies. DAPI-stained nuclei are blue; scale bar, 100 μm. Arrows point to necrotic fibers invaded by phagocytes.

Figure S3. Immunohistochemistry for LC3 (**A**) or SQSTM1 (**B**) on formalin-fixed, paraffin-embedded muscle tissue from a human patient with no obvious muscle disease. Scale bar, 50 μm.

Figure 1

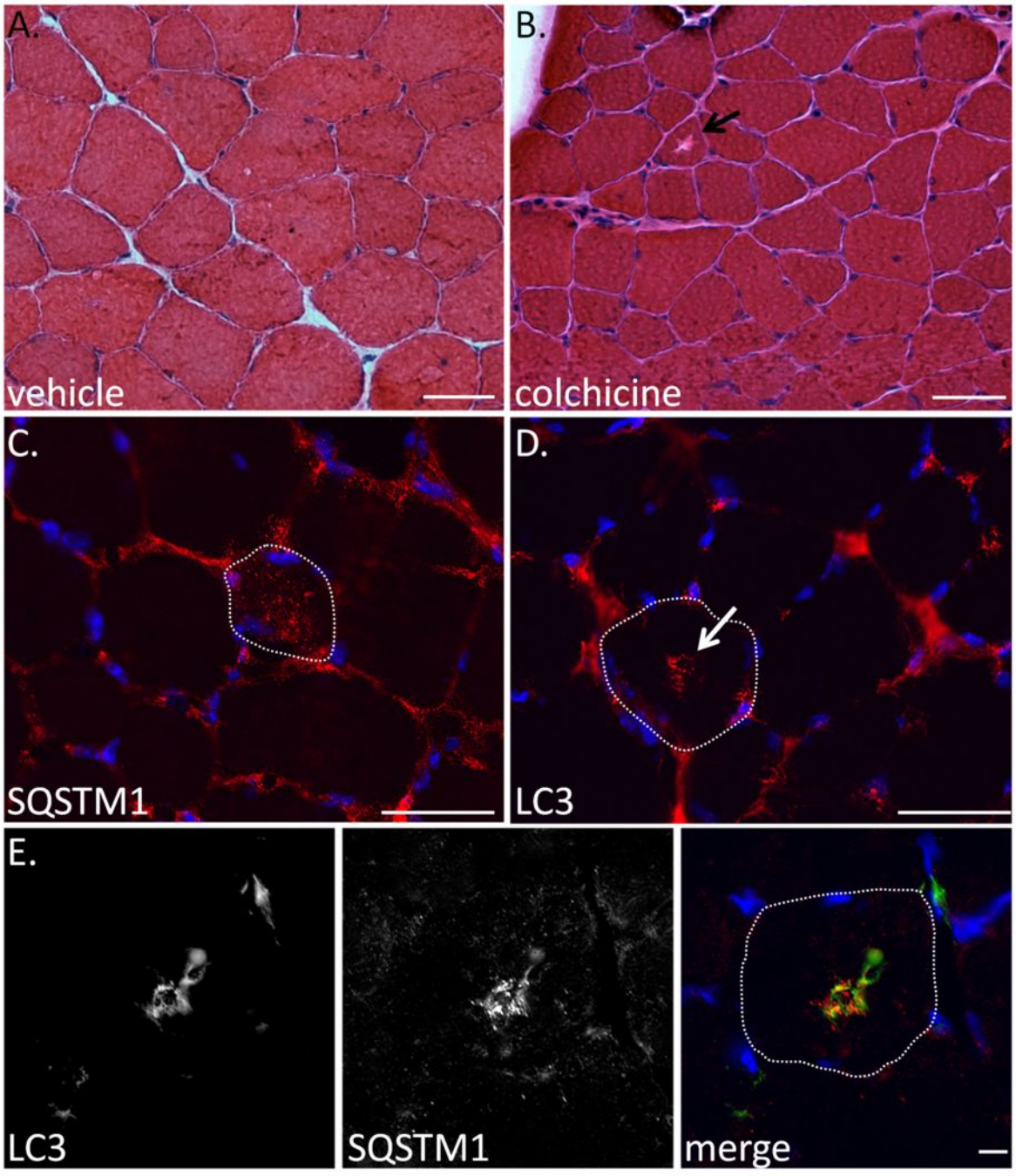

Figure 2

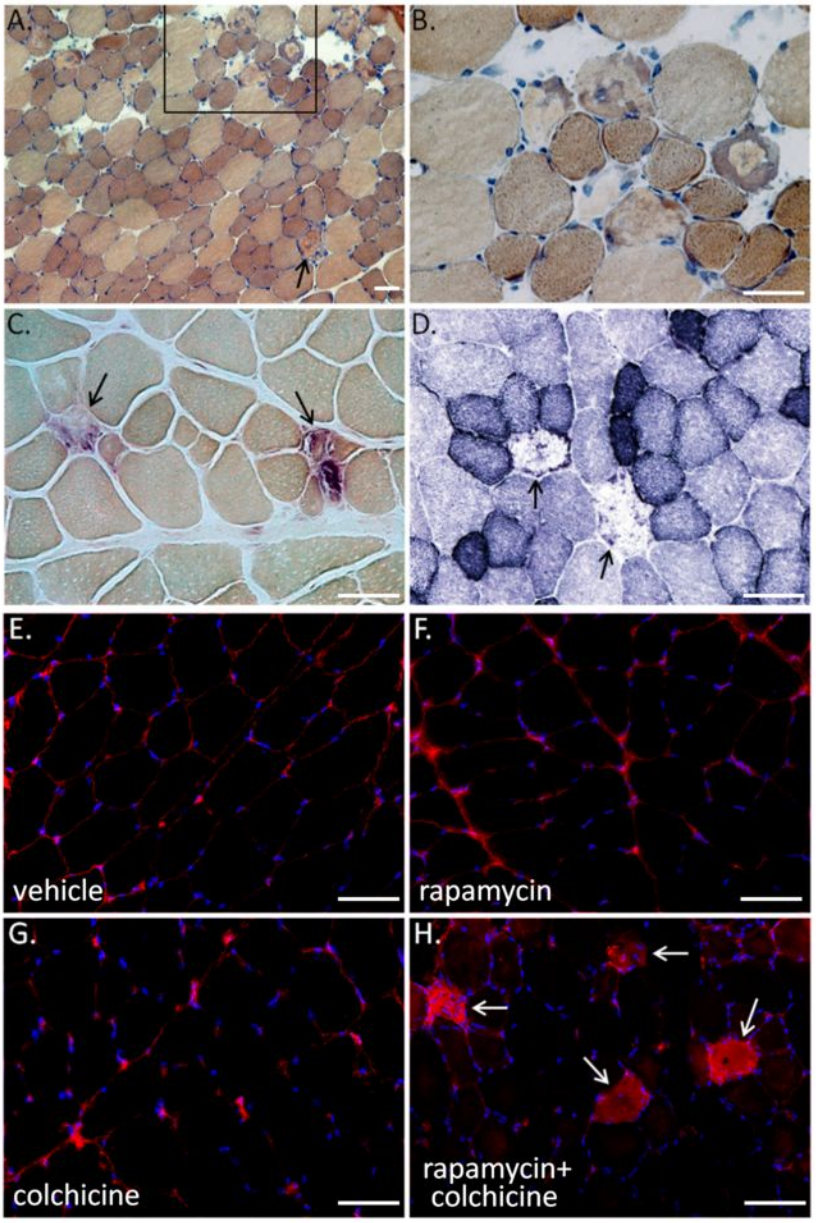
A.
B.
C.
D.
E.
vehicle
F.
rapamycin
G.
colchicine
H.
rapamycin+
colchicine

I.

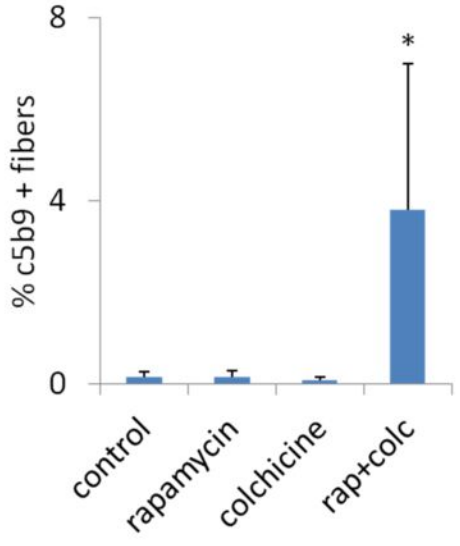
8
4
0
% c5b9 + fibers
*
control
rapamycin
colchicine
rap+colc

Figure 3:

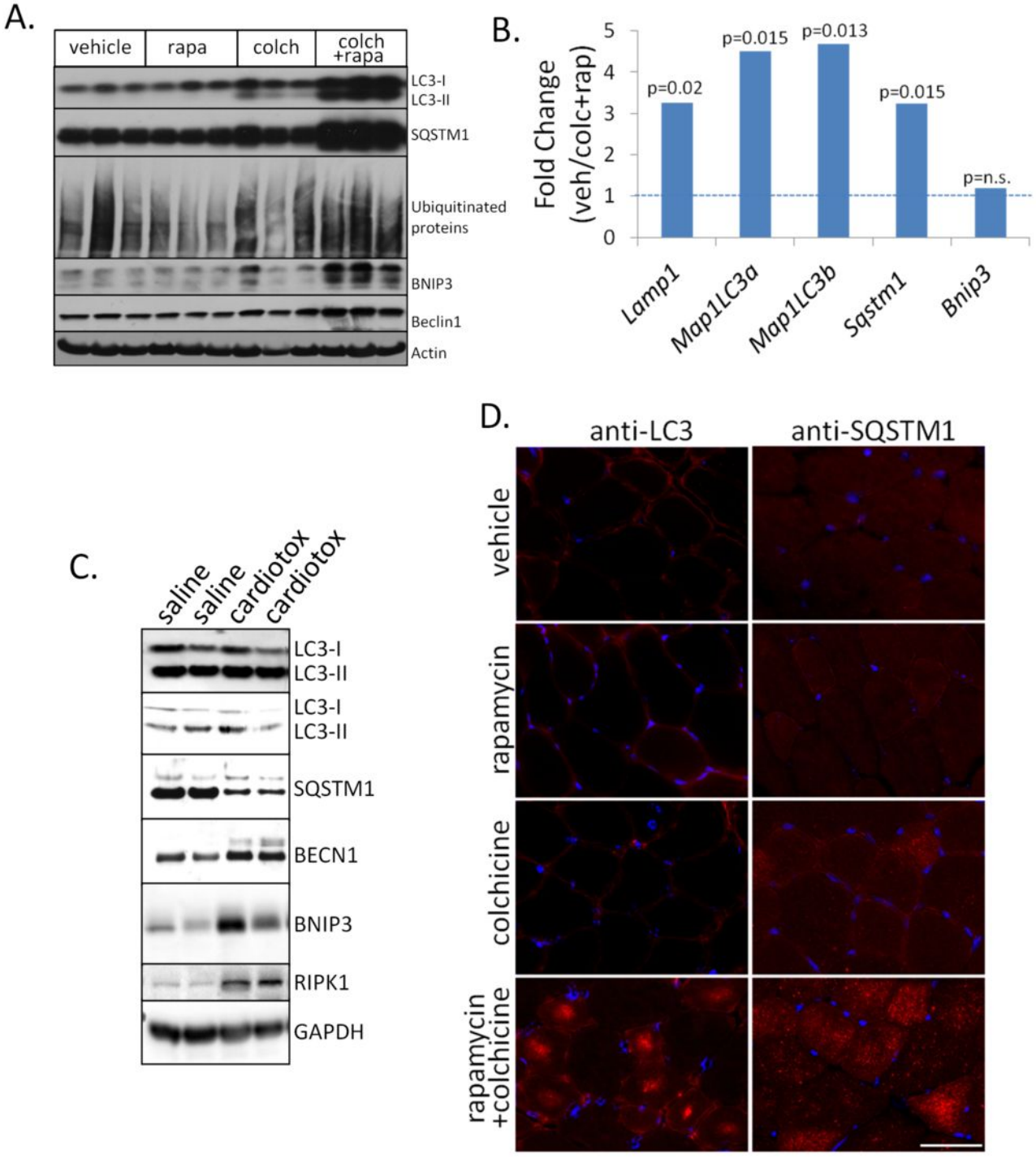
A.
vehicle
rapa
colch
colch +rapa
LC3-I
LC3-II
SQSTM1
Ubiquitinated proteins
BNIP3
Beclin1
Actin
B.
Fold Change (veh/colc+rap)
p=0.02
p=0.015
p=0.013
p=0.015
p=n.s.
Lamp1
Map1LC3a
Map1LC3b
Sqstm1
Bnip3
C.
saline
saline
cardiotox
cardiotox
LC3-I
LC3-II
LC3-I
LC3-II
SQSTM1
BECN1
BNIP3
RIPK1
GAPDH
D.
anti-LC3
anti-SQSTM1
vehicle
rapamycin
colchicine
rapamycin +colchicine

Figure 4

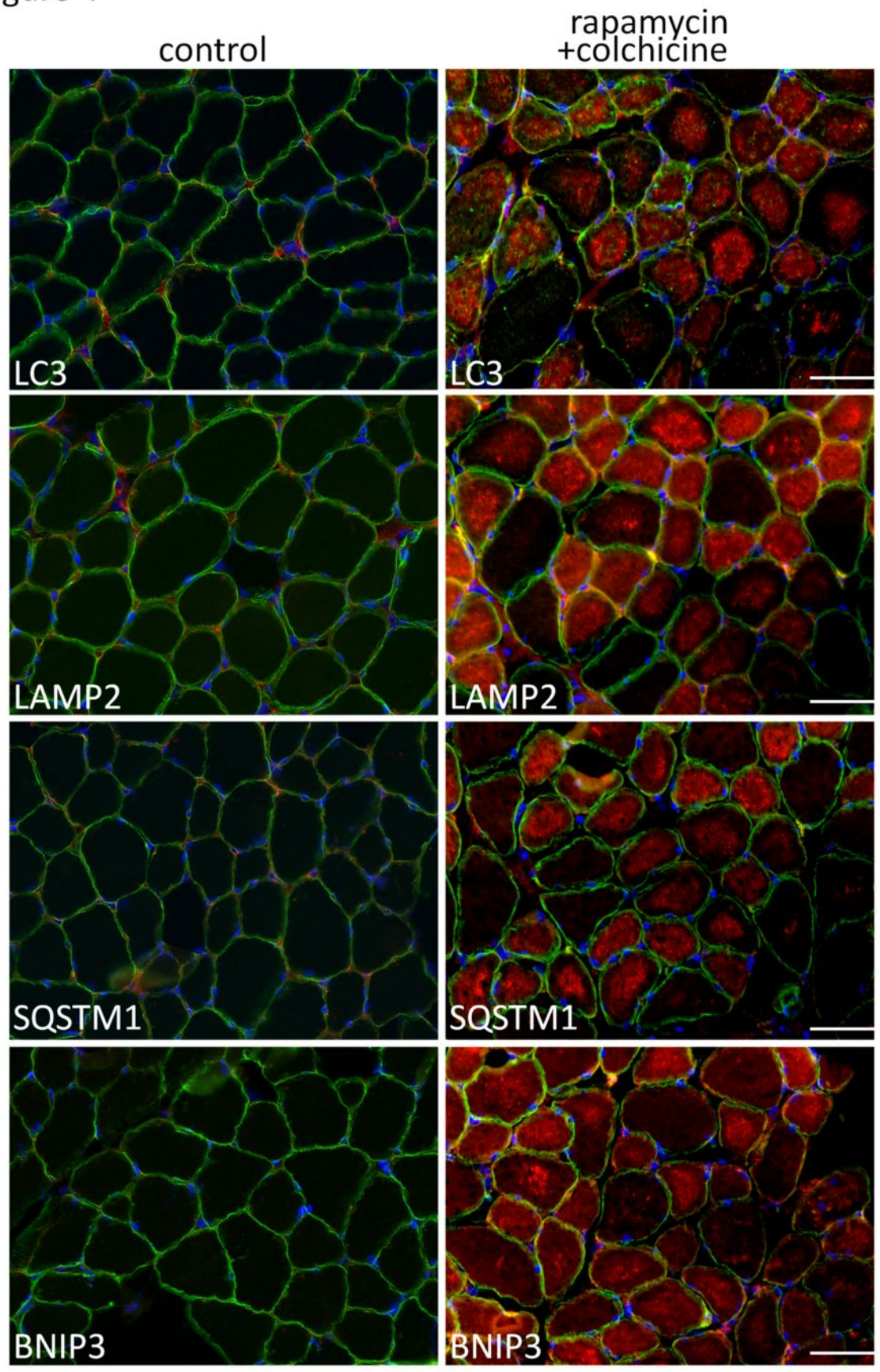
control
rapamycin
+colchicine
LC3
LC3
LAMP2
LAMP2
SQSTM1
SQSTM1
BNIP3
BNIP3

Figure 5:

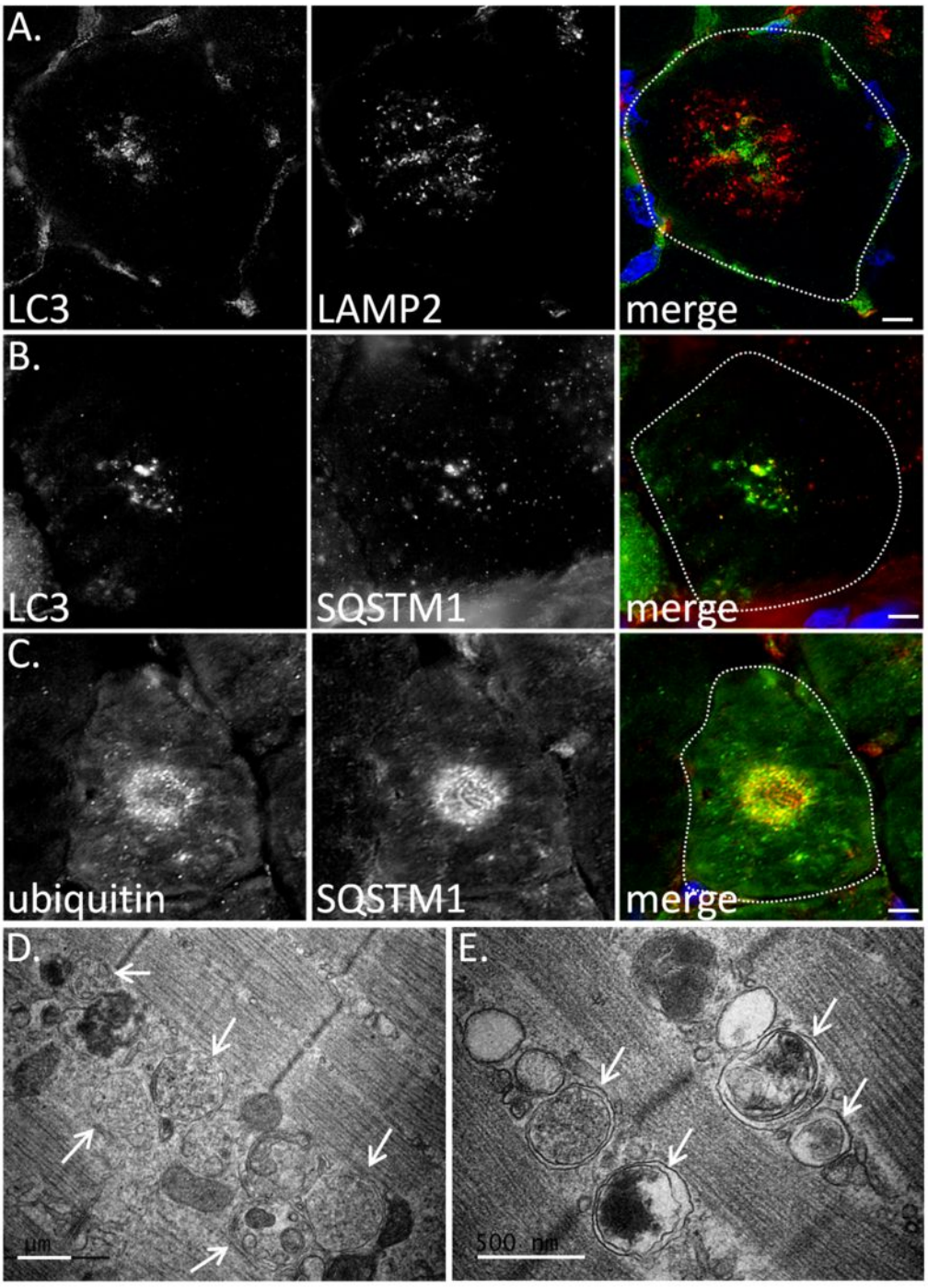
A.
LC3
LAMP2
merge
B.
LC3
SQSTM1
merge
C.
ubiquitin
SQSTM1
merge
D.
μm
E.
500 nm

Figure 6:

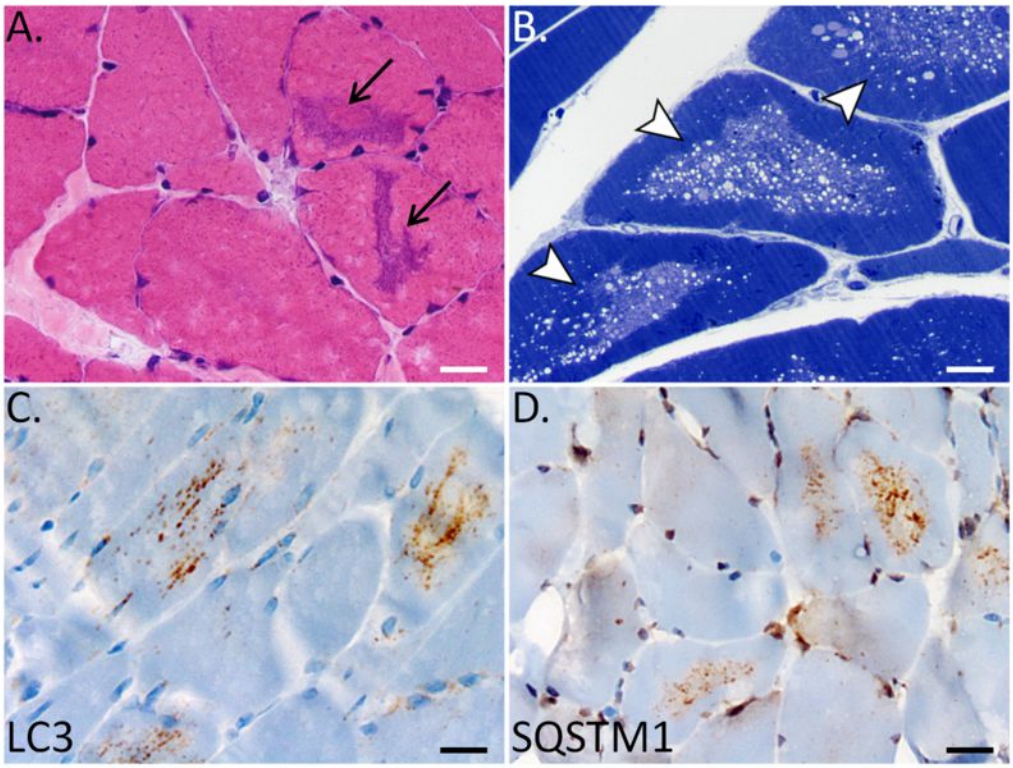

Figure 7:

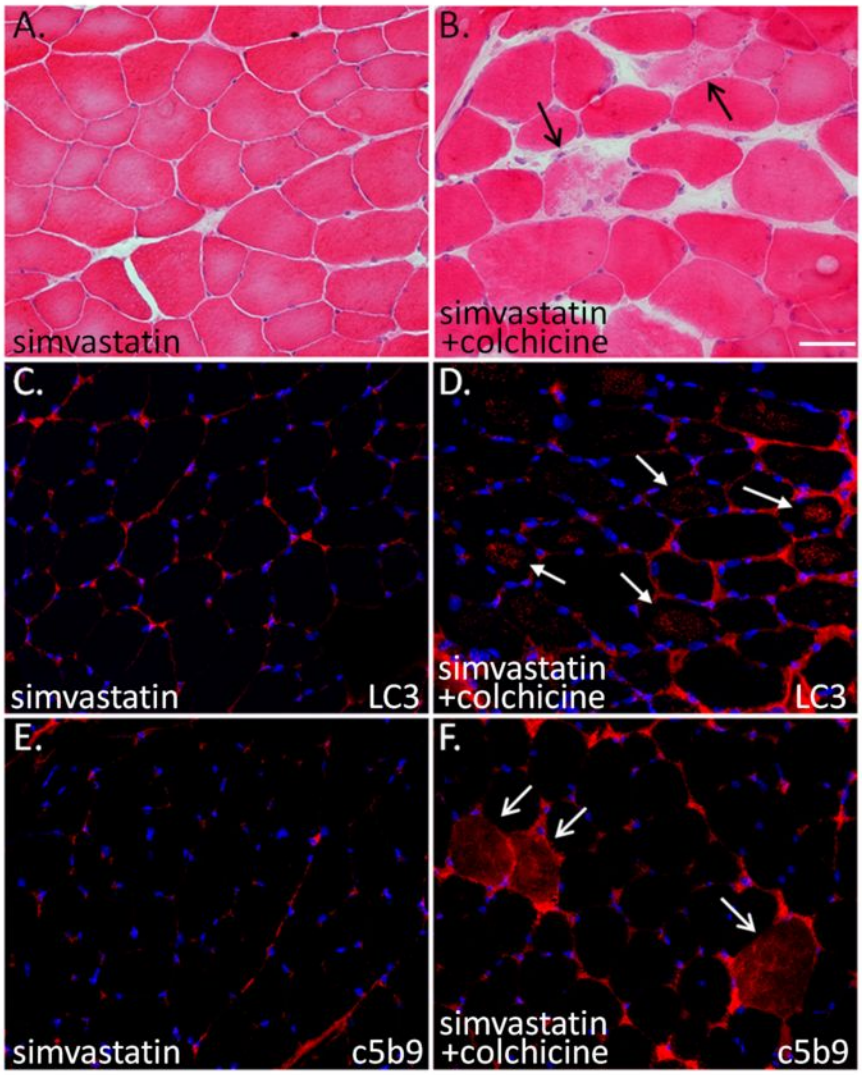
A.
simvastatin
B.
simvastatin
+colchicine
C.
simvastatin
LC3
D.
simvastatin
+colchicine
LC3
E.
simvastatin
c5b9
F.
simvastatin
+colchicine
c5b9

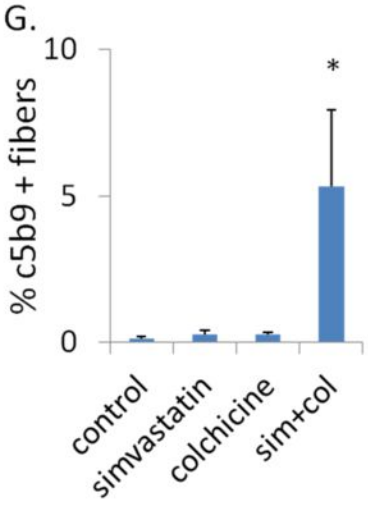
G.
% c5b9 + fibers
10
5
0
*
control
simvastatin
colchicine
sim+col

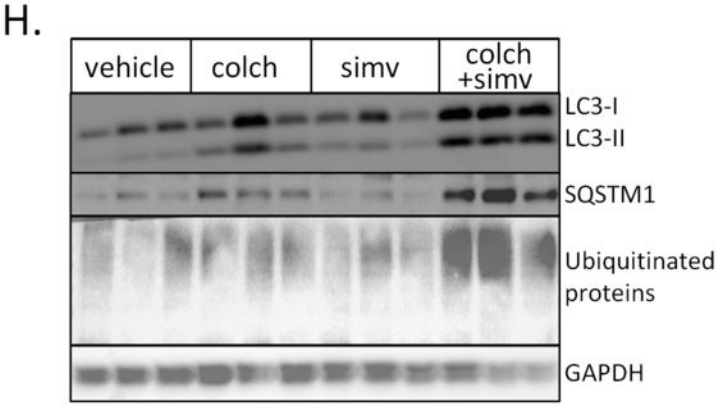
H.
vehicle
colch
simv
colch
+simv
LC3-I
LC3-II
SQSTM1
Ubiquitinated
proteins
GAPDH

Figure 8

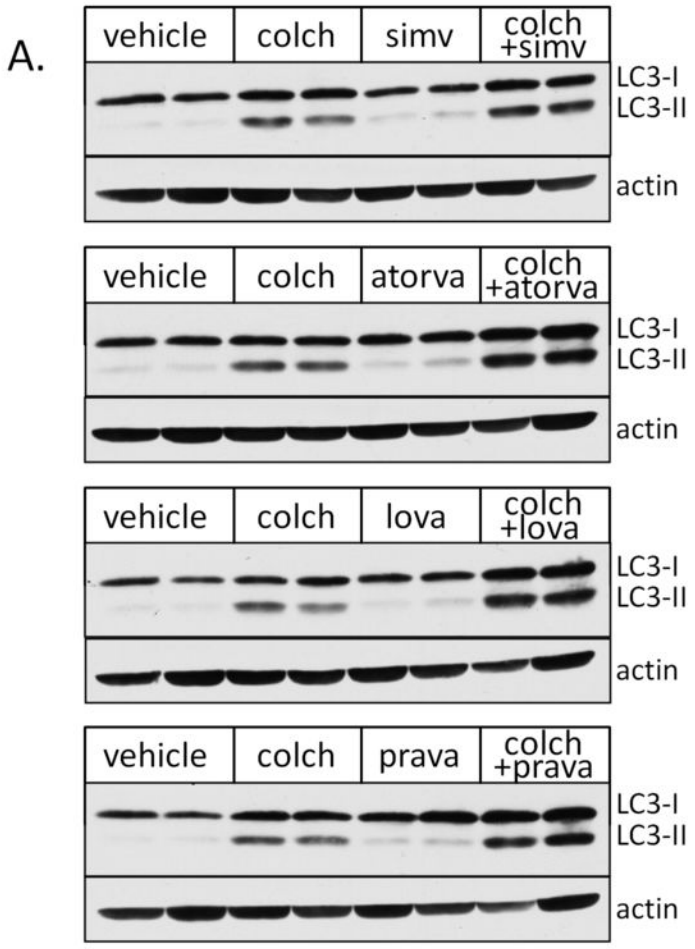
A.
vehicle
colch
simv
colch +simv
LC3-I
LC3-II
actin
vehicle
colch
atorva
colch +atorva
LC3-I
LC3-II
actin
vehicle
colch
lova
colch +lova
LC3-I
LC3-II
actin
vehicle
colch
prava
colch +prava
LC3-I
LC3-II
actin

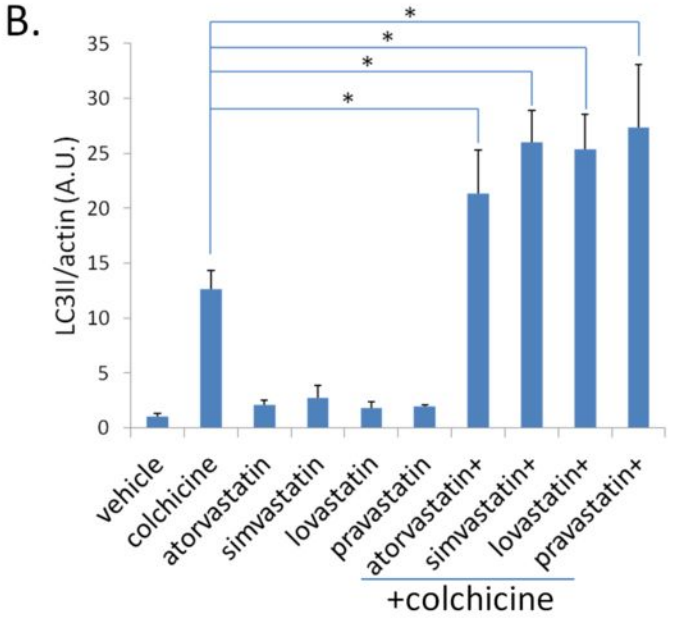
B.
LC3II/actin (A.U.)
35
30
25
20
15
10
5
0
*
*
*
*
vehicle
colchicine
atorvastatin
simvastatin
lovastatin
pravastatin
atorvastatin+
simvastatin+
lovastatin+
pravastatin+
+colchicine

Figure S1

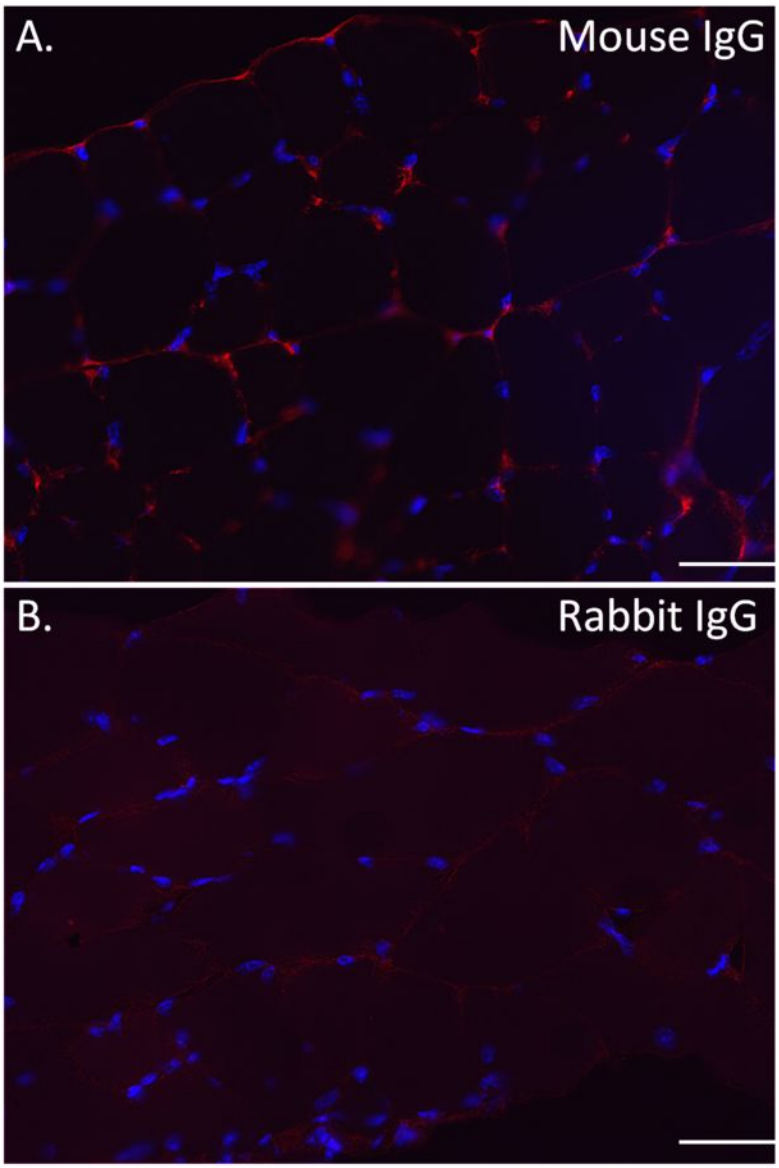

Figure S2

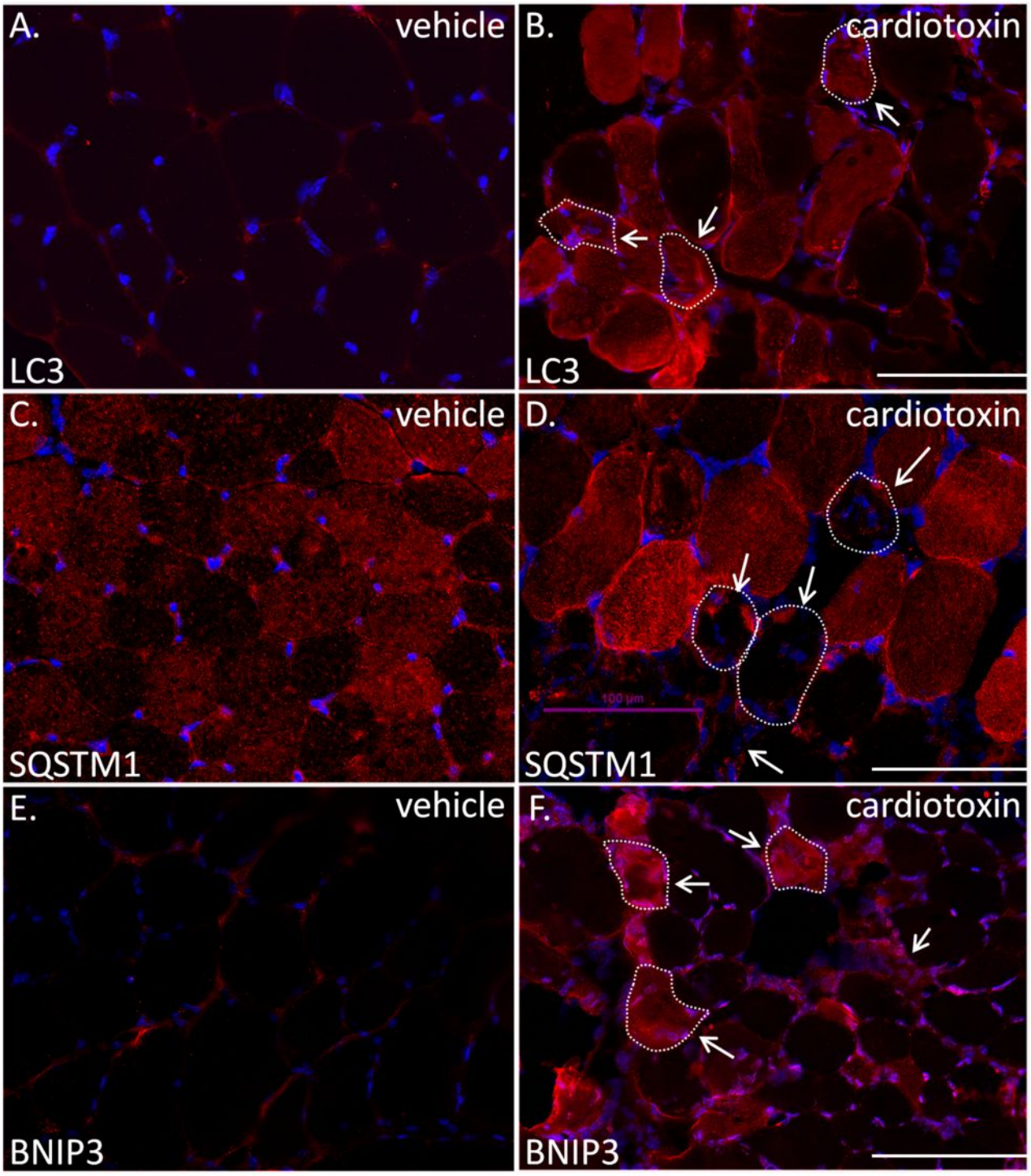
A.
vehicle
LC3
B.
cardiotoxin
LC3
C.
vehicle
SQSTM1
D.
cardiotoxin
100 µm
SQSTM1
E.
vehicle
BNIP3
F.
cardiotoxin
BNIP3

Figure S3